Research on Water Invasion Intensity of Coalbed Methane Wells Based on Material Balance Method

Yan Gao(✉), Zhong Liu, Zhi-jun Li, Xiu-qin Lu, Peng-bao Zhang, Yan-jun Chen, Yu Mao, and Zhi-kun Nie

Exploration and Development Research Institute of Huabei Oilfield Company, Renqiu, China
920984740@qq.com

Abstract. At present, many coalbed methane wells expose the problem of large water production and low depressurization efficiency which seriously affects gas production. External water supply affects adequate depressurization of coal reservoirs, impeding the desorption and output of coalbed methane and significantly reduces the gas production of coalbed methane wells. In order to evaluate the external water recharge, this paper introduces the concept of conventional oil-gas water invasion and establishes a water invasion intensity calculation model for coalbed methane wells based on the calculation of average formation pressure and the principle of material balance using dewatering data. The model quantitatively evaluates the water invasion intensity of coalbed methane well and is verified by the water head elevation and gas production rate, which is also consistent with the development of faults and aquifer. Corresponding technical measures are taken to avoid the impact of water invasion, including selecting retention and weak water invasion area for productivity construction, using area depressurization well pattern and fracturing the intervals free from water invasion. After field application, the production of low-rank and low-gas-content coalbed methane wells has made a breakthrough. The establishment of this model provides a basis for the productivity construction, well pattern design and fracturing layer selection of coalbed methane wells and has a good application prospect and promotion significance.

Keywords: Material balance equation · Water invasion intensity · Drainage and depressurization

1 Introduction

Coalbed methane production achieves "desorption-diffusion-seepage" through "drainage and pressure drop". If there is external water recharge, the water production of coalbed methane wells is large and the depressurization efficiency is low, which seriously affects the production of coalbed methane wells.

At present, there are only water invasion evaluation methods for conventional gas wells and qualitative identification methods for leakage recharge of coalbed methane wells through production curves [1–7]. There is a lack of analysis of the influence

J. Lin (Ed.): IFEDC 2023, SSGG, pp. 17–29, 2024.
https://doi.org/10.1007/978-981-97-0268-8_2

mechanism of external water on coalbed methane wells and no quantitative evaluation method has been developed for evaluation. In order to solve these problems, this paper establishes a model for calculating the water invasion intensity of coalbed methane wells by introducing the concept of conventional oil-gas water invasion and quantitatively evaluates the water invasion intensity of coalbed methane wells.

2 Influence of Water Invasion in Coalbed Methane Wells

The recharge of external water has seriously affected the production of coalbed methane wells [8–11]. Analyzed from the aspect of reservoir depressurization, after the coalbed methane well is put into production, a pressure drop funnel is formed near the bottom of the well. The rocks and fluids within the range of the pressure drop funnel constantly release elastic energy, so that the fluid continuously flows into the bottom of the well [12–15]. If there is no external water recharge after the pressure reaches the flow boundary, due to the low permeability of the coal reservoir, it can be regarded as a closed boundary. With the boundary pressure and bottomhole pressure dropping at the same time, the reservoir pressure is fully depressurized and the pressure drop funnel deepens [16–18] (Fig. 1a). If the hydrodynamic condition is strong, the coalbed methane well is recharged by external water with a boundary of certain supply capacity. Thus it is difficult to achieve full depressurization of the reservoir, affecting gas desorption and production and significantly reducing the gas production of coalbed methane well (see Fig. 1b).

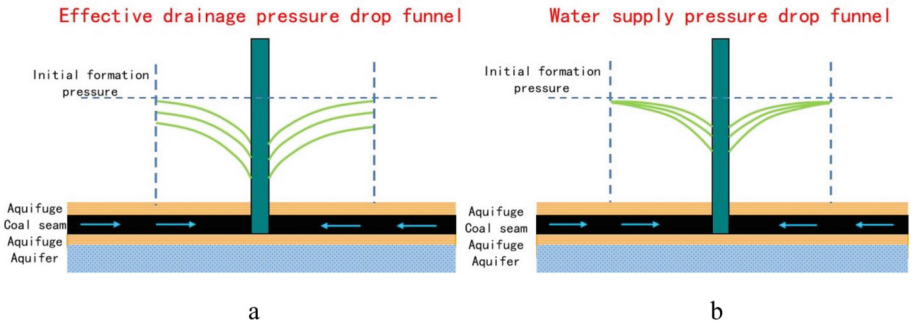

Fig. 1. Coal reservoir pressure drop funnel of effective drainage and external water recharge

3 Water Invasion Intensity Modeling

The model is built on the basis of material balance equation using dewatering data. Since the shut-in pressure measurement of coalbed methane wells affects the continuity of drainage and production, the average formation pressure cannot be obtained directly. The pressure distribution of fractured wells is calculated through the derivation of equation and the average formation pressure is converted into the expression of bottomhole flow pressure, which enables the material balance equation to be solved and the water invasion index is obtained.

3.1 Calculation of Formation Pressure Distribution in Fractured Wells

An equation is established to equate the composite radial model of fractured wells to a homogeneous model (see Fig. 2).

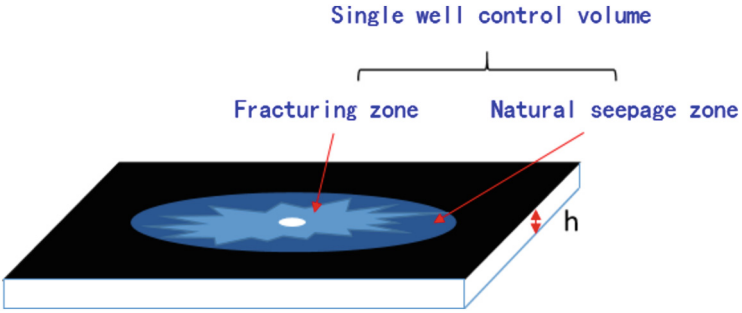

Fig. 2. Diagram of fractured coalbed methane well

Seepage equation within natural seepage zone is given below:

$$P_e - P_1 = \frac{\mu_w B_w q_w}{2\pi k_2 h} \ln \frac{r_e}{r_s} \tag{1}$$

Seepage equation in fractured area can be expressed as:

$$P_1 - P_{wf} = \frac{\mu_w B_w q_w}{2\pi k_1 h} \ln \frac{r_s}{r_w} \tag{2}$$

Adding two equations together yields:

$$P_e - P_{wf} = \frac{\mu_w B_w q_w}{2\pi k_2 h} \left(\ln \frac{r_e}{r_s} + \frac{k_2}{k_1} \ln \frac{r_s}{r_w} \right) \tag{3}$$

After sorting, we get:

$$P_e - P_{wf} = \frac{\mu_w B_w q_w}{k_2 h} \ln \frac{r_e}{r_s \frac{r_s}{r_w})^{-\frac{k_2}{k_1}}} \tag{4}$$

Equivalent radius of wellbore is.

$$r'_w = r_s \frac{r_s}{r_w})^{-\frac{k_2}{k_1}} \tag{5}$$

3.2 Calculation of average formation pressure

For fractured coalbed methane wells, the pressure reaches the flow boundary after a period of time. Since the original permeability of the coal seam is very low, the flow

beyond the natural seepage zone can be regarded as a closed boundary. Thus the flow after transmission to the boundary can be regarded as a pseudo-stable flow.

The average formation pressure is calculated by the area-weighted method:

$$\bar{p} = \frac{\int pdA}{A} = \frac{\int_{r'_w}^{r_e} p \cdot 2\pi r dr}{\pi(r_e^2 - r'^2_w)} \tag{6}$$

The expression of average formation pressure can be obtained after integration:

$$\overline{p} = p_{wf} + \frac{q_w \mu_w B_w}{2\pi k_w h}(\ln \frac{0.472 r_e}{r'_w}) \tag{7}$$

Substituting the equivalent wellbore radius, we get:

$$\overline{p} = p_{wf} + \frac{q_w \mu_w B_w}{2\pi k_w h} \ln\left(\frac{r_e}{r_s(\frac{r_s}{r_w})^{-\frac{k_2}{k_1}}} - \frac{1}{2}\right) \tag{8}$$

where, p_e is the boundary pressure, Pa; p_1 is the boundary pressure of transformation area, Pa; p_{wf} is the bottom-hole pressure, Pa; k_1 is the permeability in the reformed area, m^2; k_2 is the permeability in natural seepage zone, m^2; r_e is the control radius, m; r_s is the radius of fractured area, m; r_w is the wellbore radius, m.

3.3 Establishment of Single-Phase Flow Material Balance Equation

According to the single-phase flow material balance equation, the cumulative water production at the drainage stage is equal to the sum of fluid volume changes in the reservoir [19–21].

$$W_p B_w = C_t V(p_i - \overline{p}) + W_e \tag{9}$$

Substituting the average formation pressure expression (7), Eq. (10) can be changed to be:

$$p_{wf} = p_i - \frac{W_p B_w}{C_t V} + \frac{W_e}{C_t V} - \frac{q_w \mu_w B_w}{2\pi k_w h} \ln\left(\frac{r_e}{r_s(\frac{r_s}{r_w})^{-\frac{k_2}{k_1}}} - \frac{1}{2}\right) \tag{10}$$

3.4 Calculation of water invasion intensity

It can be seen from Eq. (10) that when the production remains stable, the fourth term on the right side of the equation is a constant, and if there is no water invasion, W_p has a linear relationship with p_{wf}.

$$p_{wf} = mW_p + b \tag{11}$$

where, m is the slope of the straight line segment of the p_{wf}-W_p correlation curve and b is the intercept of the straight line segment.

$$m = -\frac{B_w}{C_t V} \tag{12}$$

$$b = p_i - \frac{q_w \mu_w B_w}{2\pi k_w h} \ln\left(\frac{r_e}{r_s\left(\frac{r_s}{r_w}\right)^{-\frac{k_2}{k_1}}} - \frac{1}{2}\right) \tag{13}$$

From the derivation of the above equation, it can be seen that the relationship between p_{wf} and W_p of wells without water invasion is a straight line. The stronger the water invasion, the more the p_{wf}- W_p curve deviates from the straight line. The water invasion intensity is evaluated by the water invasion index when the flow pressure at the bottom of the well is reduced by 0.5MPa.

As shown in Fig. 3, the bottom-hole pressure drop by 0.5MPa is recorded as p_{wf1} and its corresponding actual cumulative water production W_{p1} is read. Assuming that no water invasion has occurred, p_{wf1} can be substituted into Eq. (11) to calculate its pure elastic drive water production W'_{p1}. Then the water influx is W_{p1}-W'_{p1} and the water invasion index can be calculated by Eq. (14).

$$WEDI = \frac{W_{p1} - W'_{p1}}{W_{p1}} \tag{14}$$

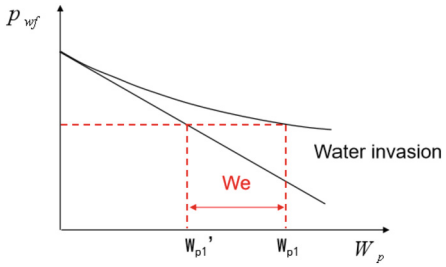

Fig. 3. Schematic diagram of water invasion index calculation

4 Case Analysis and Result Validation

The production curve of well X13 is shown in Fig. 4. According to the production data of the drainage stage, the scatter diagram of the bottom-hole flowing pressure and cumulative water production is drawn (see Fig. 5). According to Eq. (11), pure elastic drive water production is calculated: $W'_{p1} = (4.08 - 3.55)/0.003257 = 161.0\,m^3$. The actual cumulative water rate W_{p1} is 241.3 m^3 and the water invasion index with the pressure reduction of 0.5MPa is calculated using Eq. (14): $WEDI = \frac{241.3-161.0}{241.3} = 33.3\%$. The well is close to the recharge area with a high water head elevation and active hydrodynamic.

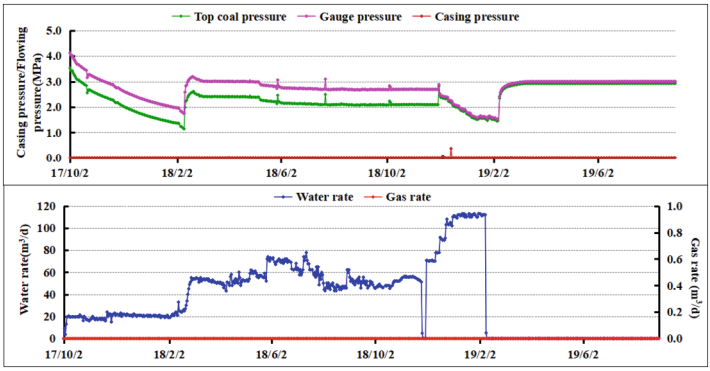

Fig. 4. Production curve of Well X13

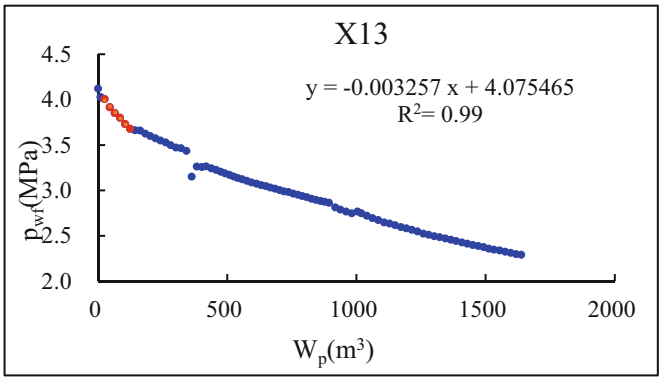

Fig. 5. p_{wf} -W_p scatter diagram and fitted straight line of Well X13.

The production curve of well X11 is shown in Fig. 6. According to the production data of the drainage stage, the scatter diagram of the bottom-hole flowing pressure and cumulative water production is drawn (see Fig. 7). The scatter diagram shows a straight line trend in the drainage stage of the well, meaning no water invasion occurs.

The drainage curve of well X1–3 is shown in Fig. 8. According to the production data in the drainage stage, the scatter diagram of the bottom-hole flowing pressure and cumulative water production is drawn (see Fig. 9). According to Eq. (11), pure elastic drive water production is calculated: $W'_{p1} = (4.36 - 3.75)/0.001071 = 572.7\,m^3$. The actual cumulative water rate W_{p1} is 241.3 m^3 and the water invasion index with the pressure reduction of 0.5MPa is calculated: $WEDI = \frac{766.1-572.7}{766.1} = 25.3\%$. According to the analysis of geological conditions, a set of aquifers developed in the upper part of the coal seam supply water to it (see Fig. 10), which is consistent with the result of a high water invasion index.

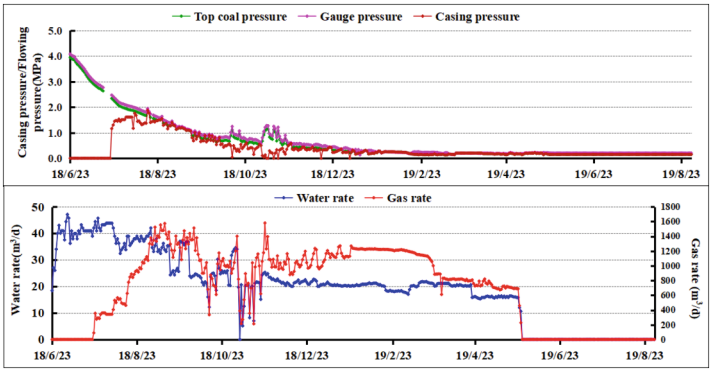

Fig. 6. Production curve of Well X11

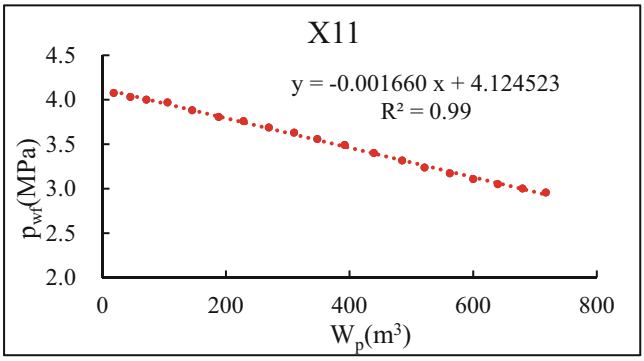

Fig. 7. p_{wf} -W_p scatter diagram and fitted straight line of Well X11.

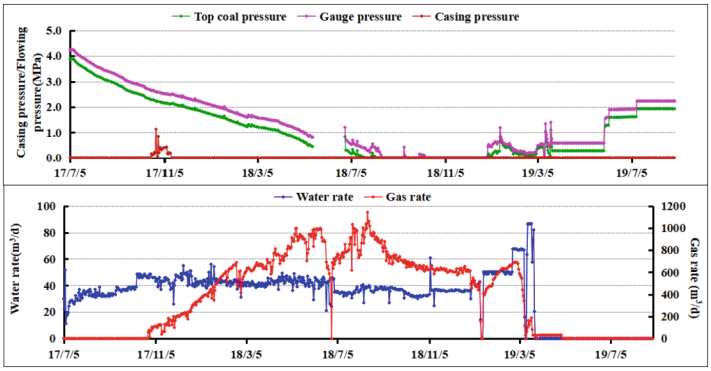

Fig. 8. Production curve of Well X1–3

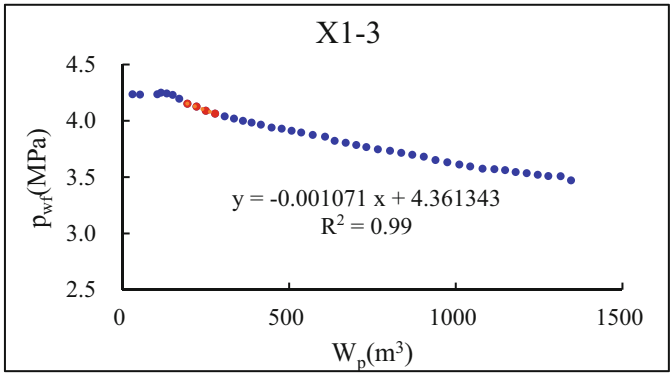

Fig. 9. p_{wf} -W_p scatter diagram and fitted straight line of Well X1–3.

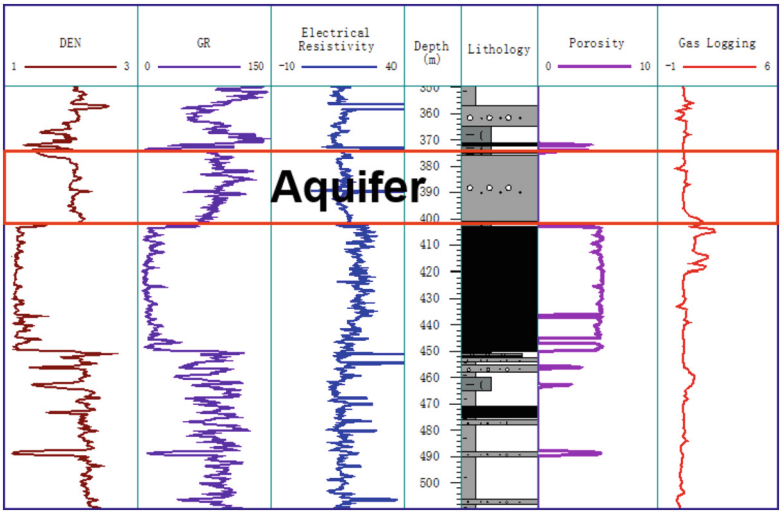

Fig.10. Four property relationship of Well X1–3

Analysis and verification are conducted according to hydrodynamic conditions. The hydrogeological environment is generally divided into three parts: recharge area, discharge area and runoff area. The runoff area can be further divided into strong runoff area, weak runoff area and retention area (see Fig. 11). The strong runoff area has strong hydrodynamic conditions, high head elevation, strong water invasion and poor gas production capacity. It can be seen from Fig. 12 and Fig. 13 that water invasion index is positively correlated with water head elevation and negatively correlated with gas production per unit pressure drop in SL Coalbed Methane Field, which verifies the model calculation results are reliable.

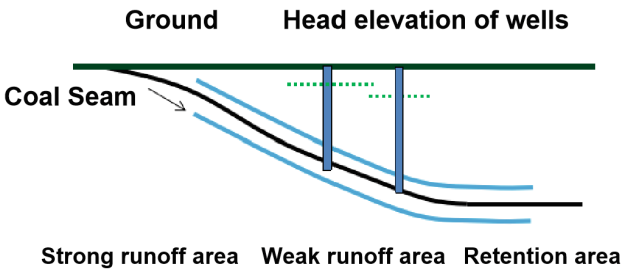

Fig. 11. Hydrodynamic conditions zoning map

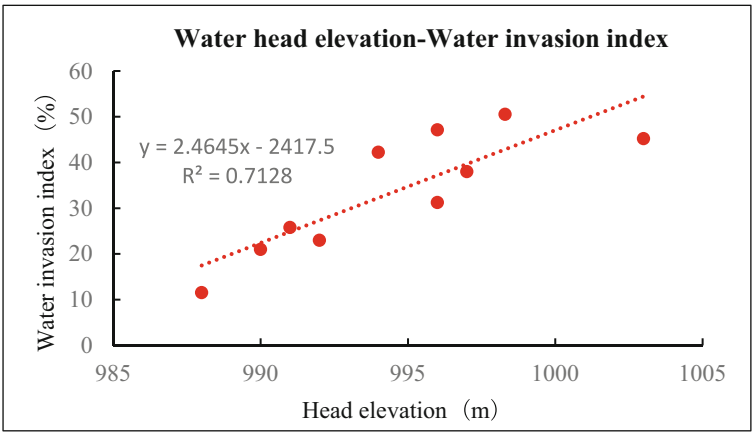

Fig. 12. Relation between water head elevation and water invasion index.

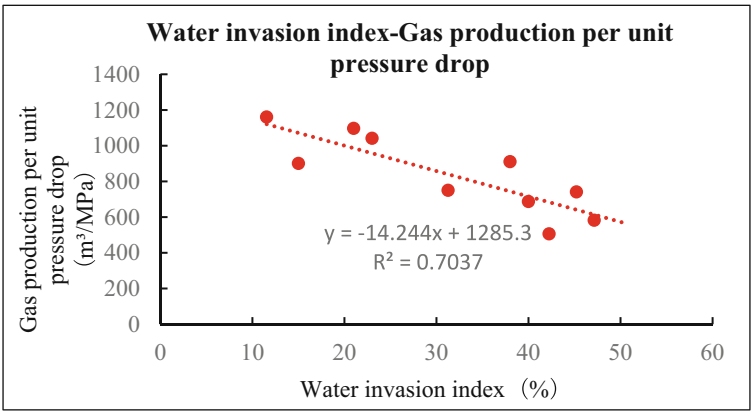

Fig. 13. Relationship between water invasion index and gas production per unit pressure drop

5 Model Application

Through the calculation of water invasion intensity model, the water invasion index distribution of wells in SL Coalbed Methane Field is obtained and the distribution map of water invasion index is drawn (see Fig. 14). From the distribution map, SL Coalbed Methane Field is divided into retention area, water invasion area of the same layer and water invasion area of the surrounding aquifer. There is no water invasion in the retention area, because the area is surrounded by faults and water cannot be supplied by the shelter from faults. Water invasion area of the same layer is the runoff area of strong hydrodynamic, where water from the same coal seam invades in the range of well controlled reserves. In the water invasion area of the surrounding rock aquifer, a set of sandstone aquifer develops at the top of coal seam and water invasion occurs under the influence of surrounding rock.

To avoid the influence of water invasion, wells should be distributed in the retention area and weak water invasion area during productivity construction, and the weak water invasion area should be explored with area-depression well pattern, which is conducive to coordinated depression between wells [22–24]. At the same time, through the well analysis of water invasion from the surrounding aquifer, there is no water invasion when the fracturing section is more than 30 m away from the bottom of the aquifer. Therefore, the fracturing perforation section should be more than 30 m away from the bottom of the aquifer when the fracturing design is carried out.

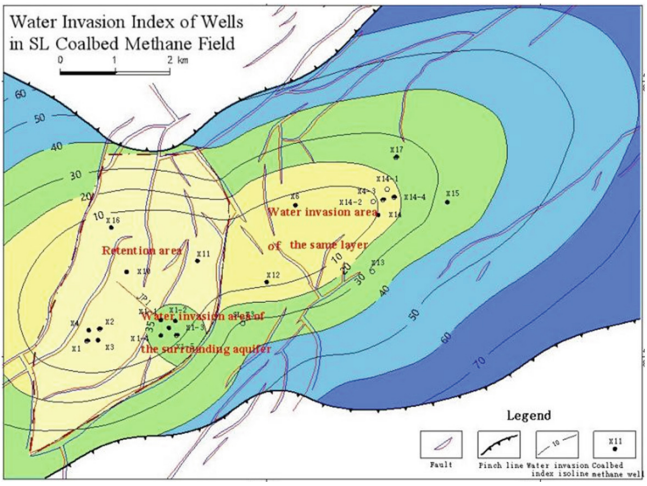

Fig. 14. Distribution of water invasion index

A vertical well JM4 and a horizontal well JP1 were deployed in the retention area. The gas production of JM4 exceeded 2400 m^3/d, and that of JP1 exceeded 3200 m^3/d in the current production promotion stage (see Fig. 15 and Fig. 16), achieving a breakthrough in the production of low-rank and low-gas-content coalbed methane wells.

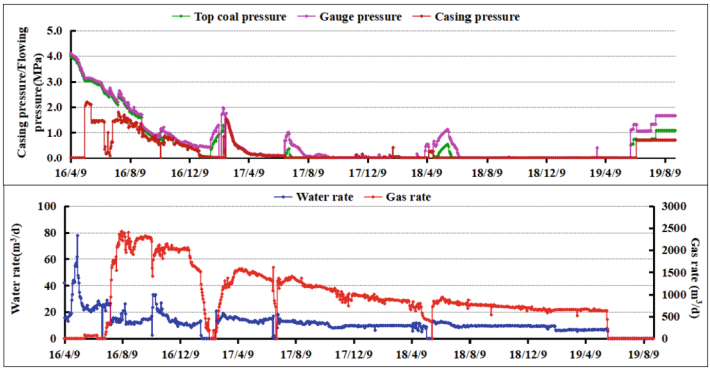

Fig. 15. Production curve of Well X4

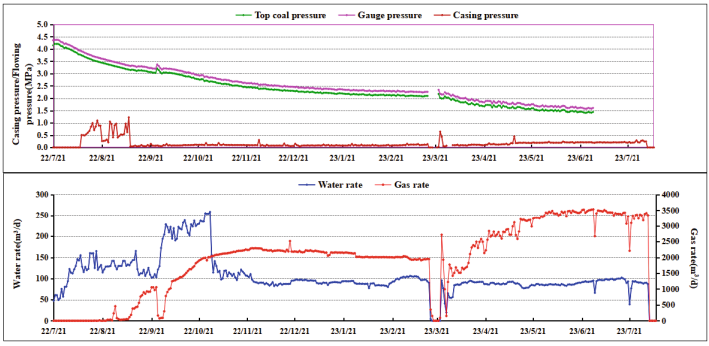

Fig. 16. Production curve of Well JP1

6 Conclusions

(1) External water recharge has serious harm to the drainage and depressurization of coalbed methane wells. Based on the principle of material balance, this paper establishes a model for calculating the water invasion intensity of coalbed methane wells and quantitatively evaluates the water supply of coalbed methane wells.

(2) The model is verified by the head elevation and the gas production capacity of wells in SL Coalbed Methane Field. The results show that the model is accurate and reliable in predicting water invasion intensity. Combined with geological understanding, the results are also consistent with the development of faults and aquifers.

(3) Through the study of water invasion intensity in SL Coalbed Methane Field, corresponding technical measures are taken to avoid the influence of water invasion. According to the zone selection method of the model, at the low gas content of 3 m^3/t, the gas production of a vertical well in the retention area has exceeded 2,400 m^3/d and that of a horizontal well has reached 3200 m^3/d in the production promotion stage, achieving a breakthrough in the gas production of low-rank coalbed

methane wells. The establishment of the model provides a basis for the zone selection of productivity construction, well pattern design and fracturing layer selection of coalbed methane wells.

References

1. Aihua, L., et al.: Water invasion identification and water production mode in gas well in Puguang gas field. Spec. Oil Gas **22**(3), 125–127 (2015)
2. Wei, S., et al.: Material balance method for the fractured water flooding gas reservoir in case of considering the water invasion strength. PGRE **16**(3), 85–87 (2009)
3. Yang, Y., et al.: Solution and typical curves of seepage model of water-bearing coal seam with leakage recharge. Coal Geol. Explor. **22**(3), 95–99 (2015)
4. Zhang Shuangbin, S., Xianbo, G.H.: Identifying method of leakage recharge in CBM wells [J]. Coal Geol. Explor. **41**(5), 30–32 (2013)
5. Xinzheng, Z., et al.: A new method for water invasion performance prediction in the early stage of fractured and water-carrying gas reservoir development [J]. J. Southwest Petrol. Univ. **29**(5), 82–85 (2007)
6. Tan, X., et al.: Material balance method and classification of non-uniform water invasion mode for gas reservoirs with water considering the effect of water sealed gas [J]. Nat. Gas Ind. (in Chinese), **41**(3), 97–103 (2021)
7. Yuanjin, P., et al.: A new model of material balance for the fractured gas reservoirs with aquifers [J]. Nat. Gas. Ind. **27**(2), 81–83 (2007)
8. Xiaodong, W., et al.: Productivity prediction of coal-bed gas wells [J]. Nat. Gas. Ind. **24**(8), 82–84 (2004)
9. Okuszko, K.E., Gault, B.W., Mattar, L.: Production decline performance of CBM wells [J]. J. Can. Petrol. Technol. **47**(7), 1–16 (2008)
10. Aminian, K., et al.: Type curves for coalbed methane production prediction[C]. In: Society of Petroleum Engineers. SPE Eastern Regional Meeting, Charleston, West Virginia, SPE-91482-MS (2004)
11. Wang, X., Zhao, Y., Wu, T.: Analysis of typical production mechanism and characteristics of coalbed methane wells for high rank coal in south Qinshui basin [J]. Coal Geol. Explor. **37**(5), 5–9 (2009)
12. Qixin, W.: Research on Storage and Transportation Law and Resource Prediction of Coalbed Methane in Fuxin Basin [D], pp. 69–71. Liaoning Technical University, Fuxin (2005)
13. Yong, Q., Yong, Z.: Evaluation and Production Technology of Methane Reservoir in Coal Seam [M], pp. 5–9. China University of Mining and Technology Press, Xuzhou (1996)
14. Weidong, Z., Qingchun, M., Wei, W.: Prospect of technology for exploration and development of CBM [J]. China Coalbed Methane **6**(5), 11–13 (2009)
15. Chuanliang, L.: Principles of Reservoir Engineering [M], pp. 150–156. Petroleum Industry Press, Beijing (2011)
16. Zhao, J., Zhang, S.: Research on pressure drop propagation law of coalbed methane drainage [J]. Coal Sci. Technol. **40**(10), 65–68 (2012)
17. Haiyang, H., et al.: Effects of pressure drop funnels model of different shapes on CBM well productivity [J]. Coal Geol. Explor. **47**(3), 109–116 (2019)
18. Du, C., et al.: Study on reservoir pressure transmission feature of coalbed methane under condition of multi-well exploitation coal science and technology [J]. Coal Sci. Technol. **44**(12), 179–183 (2016)
19. Xue, C., Cao, W., Zhong, Y.: Natural Gas Exploration and Development **23**(4), 44–49 (2000)

20. Jian, Z., Zhiming, W.: Application of material balance method in production performance prediction of coalbed methane reservoirs [J]. Coal Geol. Explor. **37**(3), 23–26 (2009)
21. Chuandong, Y., Sang, Y.: Application of material balance method in productivity prediction of coalbed methane Wells [J]. Drill. Prod. Technol. **23**(4), 33–37 (2000)
22. Xia, Y., et al.: Research on well interference of coalbed methane wells and its application [J]. Lithol. Reservoirs **27**(2), 126–132 (2015)
23. Zhang, S., et al.: Study on interference well test technology between coalbed methane wells [J]. Coal Sci. Technol. **43**(12), 75–79 (2015)
24. Fengpeng, L., et al.: Dynamic prediction method of coalbed methane well under consideration of inter-well interference [J]. J. China Univ. Min. Technol. **42**(2), 251–256 (2013)